Hyper-Raman Scattering Observation of the Boson Peak in Vitreous Silica

B. Hehlen,[1] E. Courtens,[1] R. Vacher,[1] A. Yamanaka,[2,3] M. Kataoka,[2] and K. Inoue[2]

[1]*Laboratoire des Verres, UMR 5587 CNRS, Université Montpellier 2, F-34095 Montpellier, France*
[2]*Research Institute for Electronic Science, Hokkaido University, Sapporo 060-0812, Japan*
[3]*Chitose Institute of Science and Technology, Chitose 066-8655, Hokkaido, Japan*

(Received 25 January 2000)

Hyper-Raman spectroscopy is used to investigate low frequency vibrations of various silica glasses. A strong boson peak is observed. The corresponding modes are inactive in infrared and Raman spectra, and are nonacoustic in nature. The shape of this boson peak essentially matches the total density of vibrational states (DOS), with a constant coupling coefficient C. This and other indications suggest that these modes actually dominate the DOS of silica.

PACS numbers: 63.50.+x, 78.30.Ly, 78.35.+c

A central question on glasses is that of their structure at intermediate length scales of $\sim$10 to $\sim$50 Å. For technical reasons, this cannot be addressed with the usual structural analysis methods [1]. However, this structure affects the vibrational spectrum at sufficiently low frequencies ω. Hence, the great interest in the boson peak. This is a low-ω spectral component, first observed in Raman scattering (RS) [2–4], much investigated in inelastic neutron scattering (INS) [5–7], but whose origin remains debated. As its name indicates, it obeys Bose-Einstein statistics, while thermal relaxations do not. Its position in ω corresponds to the excess specific heat and to the plateau in the thermal conductivity [4], which are universal features of glasses observed at about 10 K. It also seems to correspond to the apparent onset of strong scattering of acoustic phonons, i.e., to the end of what can rightly be called acoustic branches [8]. The interest in observing this ω region with hyper-Raman scattering (HRS) is that the selection rules are distinct from these of RS and infrared (IR) spectroscopies [9]. In HRS two photons are absorbed for one emitted; all IR-active modes are allowed, but there are modes silent both in IR and in RS that are active. Furthermore, in systems of sufficiently high symmetry there is mutual exclusion between RS and HRS. It is of obvious interest to investigate the presence of a boson peak in HRS from glasses, and to compare the results to those of other spectroscopies.

HRS from glasses, pioneered by Denisov *et al.* [9,10], is a technically demanding experiment, the signal being typically $\sim 10^6$ times smaller than in RS. The early work was limited in resolution, and the very extensive results on glasses did not include the low-ω region in the wings of the intense elastic or quasielastic second harmonic scattering. Charge-coupled devices (CCDs) now allow one to achieve resolutions comparable to those of RS, with reasonable acquisition times. In this Letter, we report the first HRS observation of boson peaks in various forms of vitreous silica. The results are compared to those for the lowest TO-LO pair [11] measured in the same experiment at $\sim$460–510 cm^{-1}. It is shown that the boson peak and the TO-LO pair obey very different selection rules. This, and a comparison to other spectroscopies, allows one to propose an assignment for the boson peak observed in silica with HRS. The latter, which is distinct from the peak in RS, also seems to have the major weight in the vibrational density of states (DOS) in that ω region.

HRS was excited at 1.064 μm wavelength with the $\sim$100-ns-long pulses from a Q-switched Nd:YAG laser of 1 kHz repetition rate. The average power was $\sim$1.4 W. The beam was sharply focused with a $f = 1.8$ cm lens, to a $\sim$30 μm diameter waist in the sample. The polarization of the incident light was fixed (V), and that of the scattered light could be selected with an analyser (V or H), which could also be removed to increase the signal ($V + H$). A quarter wave plate was placed after the analyzer to avoid spurious polarization effects, allowing a quantitative comparison of VV- and VH-scattering efficiencies. The hyper-Raman signal was dispersed with a single grating monochromator of $\sim f/5$ aperture, and detected with a liquid N_2-cooled CCD camera. The spectral resolution is 5 cm^{-1} full width at half maximum, as seen from the second harmonic signal (SHS in Fig. 1a). Measurements on either tetrasil vitreous silica (υ-SiO_2) or densified silica (d-SiO_2) with $\rho = 2.43$ g/cm^3 [12] were performed at room temperature. The OH content of both samples is negligible (below 3 ppm), as checked with IR transmission of the 2.73 μm OH band.

Figure 1a shows the HRS intensity, $I(\omega)$, of υ-SiO_2 after standard data treatment, with frequencies in wave numbers $\omega/2\pi c$. It is compared to a RS spectrum of the same sample, in the same geometry. The latter was obtained with 5145 Å excitation, dispersed with a Jobin-Yvon triple monochromator, and detected with a CCD camera. The shapes of the HRS and RS signals are obviously very different. RS is dominated by the band at R, due to the symmetric stretch [13] (or "rocking" [14]) of bridging O atoms. As already known [9], there is no corresponding component in HRS. The TO-LO pair observed in that region is inactive in RS. Its near coincidence with R is accidental [13]. The D_1 and D_2 lines in RS are assigned to vibrations of small rings [15], also not seen in HRS. Figure 1b is a semilog presentation of ϵ''/ω derived from IR

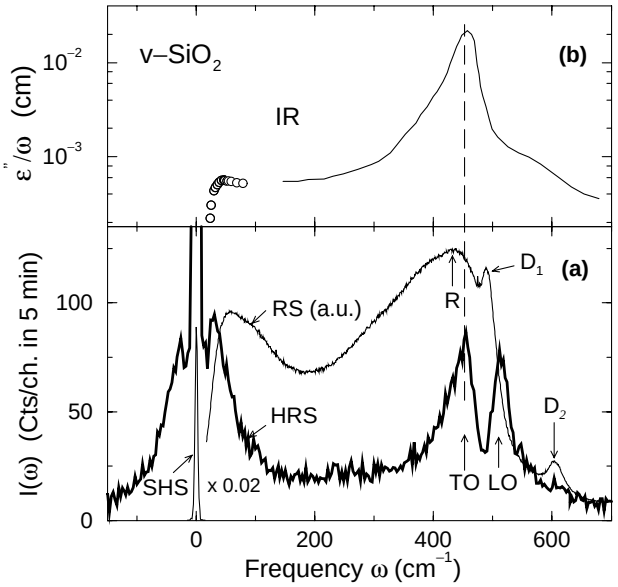

FIG. 1. Spectra of v-SiO_2: (a) Intensities of hyper-Raman (HRS) and Raman (RS) scatterings at 90° in $(V + H)$. The ordinate is for the HRS signal; (b) the imaginary part of the dielectric constant divided by ω from IR reflectivity ([16], solid line) and absorption ([17], open dots) on a semilog scale.

measurements, where ω is also in wave numbers. This is the quantity to be compared to $I(\omega)/(n + 1)\omega$ [$n(\omega)$ is the Bose factor] and thus to $I(\omega)$ at small ω. The high-ω part of Fig. 1b is adapted from [16], while the low-ω region is calculated from the far-IR transmission of water-free v-SiO_2 [17]. The strong peak in ϵ''/ω is the polar mode corresponding to the TO peak in HRS. At lower ω, one notes the boson-peak maximum at ~ 30 cm^{-1} in HRS, while in RS the maximum is at about twice that frequency. The spectral shapes on the high-ω side of these peaks are very different. Comparing to ϵ''/ω, it is clear that the boson peak in HRS is essentially nonpolar, being practically silent in IR.

To progress, one should consider the properties of HRS. Take an incident laser field $\mathbf{E}(\mathbf{r}, t)$, of wave vector $\mathbf{k}_i$ and frequency ω_i. It induces in the glass a space-time-dependent polarization $\mathbf{P}$,

$$P_i(\mathbf{r}, t) = \alpha_{ij}(\mathbf{r}, t)E_j + \beta_{ijk}(\mathbf{r}, t)E_jE_k + \dots . \quad (1)$$

α is the Raman tensor and β is the hyper-Raman tensor [18]. In this continuum model, both depend on the local symmetry at $\mathbf{r}$. These tensors are modulated by vibrational modes ζ, of dimensionless amplitude $W_\zeta(t) \propto e^{-i\omega_\zeta t}$. For the hyper-Raman tensor, one has

$$\beta(\mathbf{r}, t) = \beta_0(\mathbf{r}) + \sum_\zeta [\partial\beta/\partial W_\zeta](\mathbf{r})W_\zeta(t) + \dots . \quad (2)$$

$\beta_0(\mathbf{r})$ is a time-independent term producing second harmonic scattering, and $\partial\beta/\partial W_\zeta$ is a quantity whose symmetries are known for all point groups [19]. The hyper-Raman polarization leads to a scattered field at frequency $\omega_s = 2\omega_i \mp \omega_\zeta$, and wave vector $\mathbf{k}_s = 2\mathbf{k}_i \mp \mathbf{Q}$. This defines the scattering vector $\mathbf{Q}$. Obviously, β in (1) is symmetric in j, k. The quantum mechanical calculation of β shows that, for ω_i and ω_s far from electronic transitions, it is fully symmetric in i, j, k [20]. Our experimental results indicate that the LO-TO spectrum is dominated by fully symmetric scattering, while the antisymmetric scattering is known to contribute a relatively small background [10]. As usual, the spectrum is the Fourier transform of the correlation function of the scattered field, and it is thus given by a suitable projection of

$$\int \sum_\zeta \langle\{[\partial\beta/\partial W_\zeta](\mathbf{r} + \mathbf{r}')\}\{[\partial\beta/\partial W_\zeta](\mathbf{r}')\}\rangle \times \langle W_\zeta(t + t')W_\zeta(t')\rangle e^{i\omega t - i\mathbf{Q}\cdot\mathbf{r}}\, dt\, d^3\mathbf{r} . \quad (3)$$

The angular brackets are space and thermodynamic averages. The second one is proportional to the Bose factor divided by ω. Its integration over t leads to $\delta(\omega \mp \omega_\zeta)$ [21]. Summing over states of the same variety ζ, the expression is proportional to $Z_\zeta(\omega)(n + 1)/\omega$, where $Z_\zeta(\omega)$ is the partial DOS for that variety. This is just like the Raman case [21]. Which modes contribute depends of course on the first bracket. For modes that are fairly local, such as molecular vibrations, the correlation function in the first bracket is of small extent compared to $1/Q$, so that the integral over $\mathbf{r}$ is independent of $\mathbf{Q}$. For molecules it suffices to take the average of $(\partial\beta/\partial W_\zeta)^2$ over all orientations, as discussed in [19]. For glasses, $\partial\beta/\partial W_\zeta$ can be separated into its mean $\bar{\beta}$ and its fluctuations $\Delta\beta$ [10]. The mean has the properties of an isotropic medium, $\bar{\beta}_{VVV} = 3b$, and $\bar{\beta}_{HVV} = b$ [10]. It is only active for polar modes, and for these it is likely to dominate the spectrum. This is what happens for TO and LO, with a larger b value for LO owing to the electro-optic coupling with the internal field in that case [22].

Figure 2 illustrates the dependence of reduced HRS spectra, $I(\omega)/(n + 1)\omega$, on polarization and scattering angles for v-SiO_2. These are proportional to $\chi''(\omega)/\omega$, where $\chi''(\omega)$ is the imaginary part of the susceptibility. The interpretation of the TO-LO pair is fully described in the works of Denisov *et al.* [9,22]. Our improved resolution allows us to quantitatively check their analysis. In VV scattering, only the TO mode scatters, as the LO displacement does not have a component along V. Thus $I_{VV} \propto 9b_{\mathrm{TO}}^2$. In VH, both LO and TO motions project onto the H direction, so that $I_{VH} \propto \frac{1}{2}b_{\mathrm{TO}}^2 + \frac{1}{2}b_{\mathrm{LO}}^2$ at 90°. Since $b_{\mathrm{TO}}^2 \ll b_{\mathrm{LO}}^2$, the TO contribution to VH scattering is weak compared to the LO contribution, as observed. The inset shows the evolution with angle of $V + H$ scattering. In VH geometry, the LO displacement is parallel to H in near forward scattering, while it is the TO displacement which is seen in backscattering. Hence, I_{V+H} is proportional to $9b_{\mathrm{TO}}^2 + b_{\mathrm{LO}}^2$ at 0°, $9.5b_{\mathrm{TO}}^2 + 0.5b_{\mathrm{LO}}^2$ at 90°, and $10b_{\mathrm{TO}}^2$ at 180°. The relative LO and TO signals agree with the above, however, with a small background which can arise from the contributions of all other modes in this region owing to $\Delta\beta$ plus the rather weak antisymmetric scattering [10]. The spectra of v-SiO_2 and d-SiO_2

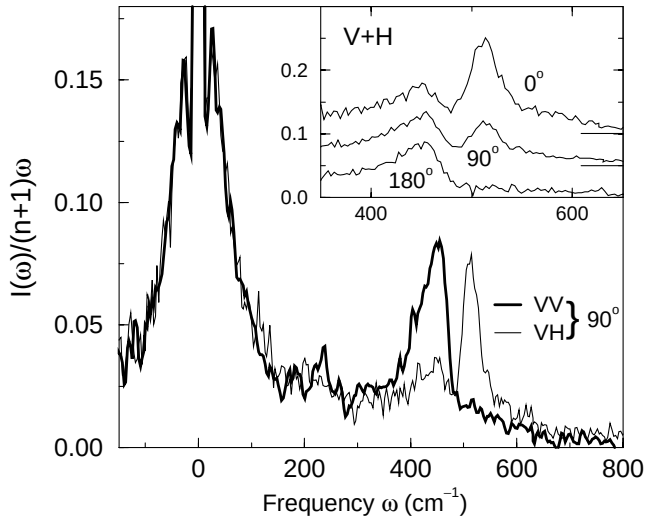

FIG. 2. Reduced hyper-Raman spectra of v-SiO_2 for different polarizations and scattering angles (inset). The curves in the inset are shifted vertically with the baselines shown.

are compared in Fig. 3. The TO mode of d-SiO_2 trails towards low frequencies. This effect was already noted in the IR spectrum of v-SiO_2 (see Fig. 1b), and it was explained by disorder [16], in particular by the distribution of Si-O-Si angles. This distribution should widen considerably upon densification, producing the broadening of the TO line seen in Fig. 3. The LO modes of both glasses practically coincide. Interestingly, there is little broadening of the LO line, possibly owing to the long-range electric field of the longitudinal mode.

We now turn to the discussion of HRS in the boson-peak region. Figure 2 shows that $I_{VH} \cong I_{VV}$, i.e., that the spectrum is fully depolarized. Hence, it cannot arise from $\bar{\beta}$ which leads to a depolarization ratio of only $1/9$. This indicates that the modes are nonpolar, also in agreement with the absence of a LO-TO splitting on the boson peak (Fig. 2) and with the very low IR absorption at low ω (Fig. 1b). One knows, in the molecular case, that the largest depolarization ratios are obtained for modes silent in IR absorption [19]. Since the shape of the HRS boson peak is so different from the RS boson peak, we conclude that the modes leading to the HRS peak are essentially silent both in IR and in RS. The local symmetry in the glass is mainly that of the SiO_4 tetrahedra T_d. In T_d, there is only one type of vibrations forbidden in IR and RS, and active in HRS [19]. These vibrations are the F_1 modes whose eigenvectors have the symmetry of the infinitesimal rotation operators. It suggests that the boson peak of HRS is principally due to modes involving rotations of SiO_4 tetrahedra [23]. This agrees with the early model of Buchenau *et al.* [5,6], and with more recent simulations [24].

One should thus compare the HRS spectrum to the total DOS, $Z(\omega)$, using $I(\omega) = C(\omega)(n + 1)Z(\omega)/\omega$, where $C(\omega)$ is a coupling parameter such as introduced in [21]. For modes that are not of acoustic type, one expects that $C(\omega) \propto \omega^0$ [21]. Then, $I(\omega)$ should directly match the average $S(Q, \omega)$ measured in INS at large values of Q. Indeed, $S(Q, \omega) \cong (n + 1)Z(\omega)/\omega$, in the "incoherent" approximation. That this comparison should be made is obvious just by considering the insets of Figs. 3 and 4. The former shows $I(\omega)$ for both v-SiO_2 and d-SiO_2, and the latter shows $S(Q, \omega)$ taken from [25], in which the line for d-SiO_2 corresponds to $\rho = 2.63$ g/cm^3. The resemblance is striking. We do not have the information on $S(Q, \omega)$ for the density $\rho = 2.43$ g/cm^3 of d-SiO_2 used here. Hence, a quantitative comparison can only be made now for v-SiO_2. The open symbols in Fig. 4 show $S(Q, \omega)$ at $Q = 2$ Å^{-1} [26]. This is essentially controlled by $Z(\omega)$, and indeed it compares well with the corresponding curve in the inset. The solid symbols are

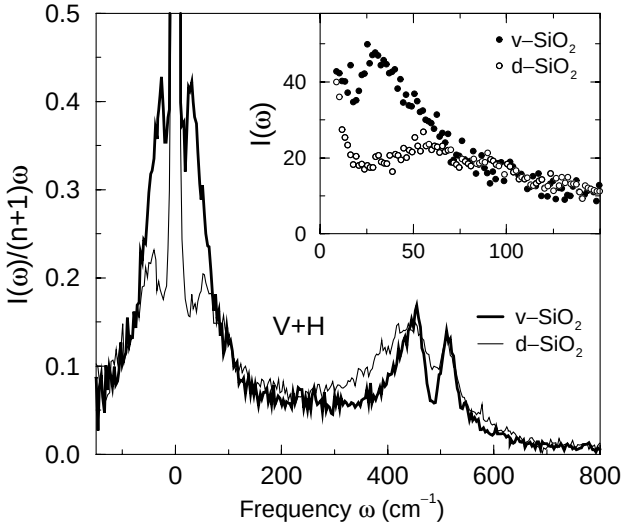

FIG. 3. Reduced hyper-Raman spectrum of v-SiO_2 and d-SiO_2. The two spectra superpose on the LO peak. The inset shows the intensities $I(\omega)$ in the boson-peak region.

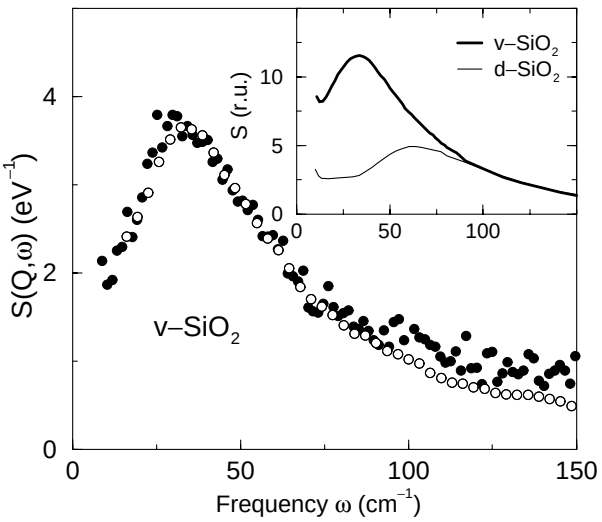

FIG. 4. Inelastic neutron structure factor (open dots) and scaled HRS intensity $I(\omega)$ (solid dots), as explained in the text. The inset shows $S(Q, \omega)$ for v-SiO_2 and d-SiO_2 from [25].

the HRS signal from which the elastic central peak was subtracted. The shape of the elastic peak is a property of the spectrometer that was measured by illuminating a scatterer with second harmonic light. For the presentation in Fig. 4, the peaks of I and S were matched. Except for the wing above $\sim 100\ \mathrm{cm}^{-1}$, the two signals superpose. An additional contribution to HRS in the high-ω wing can easily arise from other couplings (such as antisymmetric scattering) to modes which in fact do not have much weight in the DOS. Alternatively, one could subtract just a small background from the HRS spectrum, in which case it remarkably superposes $S(Q, \omega)$ over the full range of ω. We conclude that with the present data, the DOS in the region of interest can be accounted for by the modes active in HRS, and this with a *constant* C. Thus, an interpretation of $S(Q, \omega)$ in this region in terms of acousticlike excitations only (as suggested, e.g., in [26]) is not warranted.

In the present interpretation, the density of boson-peak modes seen in HRS should be much larger than that in RS. Not knowing the coupling coefficients, this cannot be checked precisely. However, an order-of-magnitude estimate of the relative strengths of RS and HRS is possible. For modes that were equally active in RS and HRS, the ratio of intensities were $I_{\mathrm{HRS}}/I_{\mathrm{RS}} \simeq (\beta E/\alpha)^2 \simeq (E/E_{\mathrm{int}})^2$, where E_{int} is an internal field characterizing the electronic binding [9]. Our relative RS and HRS intensities have been calibrated by measuring directly the RS signal with the HRS spectrometer, using second-harmonic excitation. By comparing intensities at the respective peaks, we find $I_{\mathrm{HRS}}/I_{\mathrm{RS}} \simeq 5 \times 10^{-4}$, this with $E \simeq 10^8$ V/m. If the modes were equally active in RS and HRS, this would give $E_{\mathrm{int}} \simeq 4 \times 10^9$ V/m. This is too small by about an order of magnitude. It means that I_{HRS} might in fact be as much as 2 orders of magnitude stronger than I_{RS}. Although such a comparison is only roughly quantitative, this agrees with the view that many more modes are active in HRS than in RS.

In conclusion, it appears that the vibrations that produce the boson peak in HRS are precisely those that contribute the major weight to the total DOS measured in INS. These vibrations are nonpolar. Their coupling coefficient $C(\omega)$ is constant, as opposed to $C(\omega) \propto \omega^2$ for acousticlike modes [3,27]. Hence, the DOS in the region of the boson peak is dominated by nonacoustic modes, silent in RS, while acousticlike modes may contribute to RS. This finding confirms INS results which have shown that acoustic modes, in the Debye approximation, could at most account for $\sim 20\%$ of the whole DOS in that region [6]. We also observed a strikingly similar behavior in a rather different silicate glass [28]. Hence, the main conclusions are not restricted to silica. It will be most interesting of course to observe HRS from glasses of other families to extend the understanding of boson-peak phenomena.

The authors thank Dr. M. Arai for providing the sample of d-SiO_2, Dr. J.-L. Sauvajol and Dr. E. Anglaret for their assistance in taking the Raman spectra, and Dr. M. Foret for the experimental values of $S(Q, \omega)$ used in Fig. 4.

[1] A. C. Wright, J. Non-Cryst. Solids **179**, 84 (1994).
[2] R. S. Krishnan, Proc. Indian Acad. Sci. A **37**, 377 (1953); P. Flubacher, A. J. Leadbetter, J. A. Morrison, and B. P. Stoicheff, J. Phys. Chem. Solids **12**, 53 (1959).
[3] J. Jäckle, in [4], p. 135.
[4] *Amorphous Solids, Low-Temperature Properties*, edited by W. A. Phillips (Springer, Berlin, 1981).
[5] U. Buchenau, N. Nücker, and A. J. Dianoux, Phys. Rev. Lett. **53**, 2316 (1984).
[6] U. Buchenau, M. Prager, N. Nücker, A. J. Dianoux, N. Ahmad, and W. A. Phillips, Phys. Rev. B **34**, 5665 (1986).
[7] A. P. Sokolov, Physica (Amsterdam) **219B–220B**, 251 (1996), and references therein.
[8] E. Rat, M. Foret, E. Courtens, R. Vacher, and M. Arai, Phys. Rev. Lett. **83**, 1355 (1999).
[9] V. N. Denisov, B. N. Mavrin, and V. B. Podobedov, Phys. Rep. **151**, 1 (1987).
[10] V. B. Podobedov, J. Raman Spectrosc. **27**, 731 (1996).
[11] F. L. Galeener and G. Lucovsky, Phys. Rev. Lett. **37**, 1474 (1976).
[12] A. Hiramatsu, M. Arai, H. Shibazaki, M. Tsukenawa, T. Otomo, A. C. Hannon, S. M. Bennington, N. Kitamura, and A. Onodera, Physica (Amsterdam) **219B–220B**, 287 (1996).
[13] F. L. Galeener, A. J. Leadbetter, and M. W. Stringfellow, Phys. Rev. B **27**, 1052 (1983).
[14] R. J. Bell, P. Dean, and D. C. Hibbins-Butler, J. Phys. C **4**, 1214 (1971).
[15] A. Pasquarello and R. Car, Phys. Rev. Lett. **80**, 5145 (1998).
[16] P. H. Gaskell and D. W. Johnson, J. Non-Cryst. Solids **20**, 153 (1976); **20**, 171 (1976).
[17] K. W. Hutt, W. Phillips, and R. J. Butcher, J. Phys. Condens. Matter **1**, 4767 (1989).
[18] R. W. Terhune, P. D. Maker, and C. M. Savage, Phys. Rev. Lett. **14**, 681 (1965).
[19] S. J. Cyvin, J. E. Rauch, and J. C. Decius, J. Chem. Phys. **43**, 4083 (1965).
[20] J. H. Christie and D. J. Lockwood, J. Chem. Phys. **54**, 1141 (1971).
[21] R. Shuker and R. W. Gammon, Phys. Rev. Lett **25**, 222 (1970).
[22] V. N. Denisov, B. N. Mavrin, V. B. Podobedov, Kh. E. Sterin, and B. G. Varshal, J. Non-Cryst. Solids **64**, 195 (1984).
[23] A similar assignment was made in the β phase of quartz by Y. Tezuka, S. Shin, and M. Ishigame [Phys. Rev. Lett. **66**, 2356 (1991)].
[24] S. N. Taraskin and S. R. Elliott, Phys. Rev. B **56**, 8605 (1997).
[25] Y. Inamura, M. Arai, O. Yamamuro, A. Inaba, N. Kitamura, T. Otomo, T. Matsuo, S. M. Bennington, and A. C. Hannon, Physica (Amsterdam) **263B–264B**, 299 (1999).
[26] M. Foret, E. Courtens, R. Vacher, and J.-B. Suck, Phys. Rev. Lett. **77**, 3831 (1996).
[27] A. J. Martin and W. Brenig, Phys. Status Solidi (b) **64**, 163 (1974).
[28] B. Hehlen *et al.* (to be published).